Supporting Information

HIF and HOIL-1L–mediated PKCζ degradation stabilizes plasma membrane Na,K-ATPase to protect against hypoxia-induced lung injury

Natalia D. Magnani, Laura A. Dada, Markus A. Queisser, Patricia L. Brazee, Lynn C. Welch, Kishore Anekalla, Guofei Zhou, Olga Vagin, Alexander V. Misharin, Scott G. R. Budinger, Kazuhiro Iwai, Aaron J. Ciechanover and Jacob I. Sznajder.

Experimental Procedures

Reagents. The following monoclonal antibodies were used: Na,K-ATPase subunit α_1 clone 464.6 and HOIL-1L (EMD Millipore), PKCζ clone H-1 and E-cadherin (Santa Cruz Biotechnology), GFP (Abcam), hemagglutinin (HA) clone 16B12 (Biolegend), FLAG clone M2 (Sigma) and CD29 (BD Bioscience), phospho-PKCζ/λ T410 and Lys-48 linked polyubiquitin (Cell Signaling Technology), HIF-1α (Cayman), and HOIP (Aviva System Biology), Podoplanin (T1α) (Thermo Fischer). The following polyclonal antibodies were used: SP-C (Santa Cruz Biotechnology), β-actin clone AC-15 (Sigma-Aldrich), and SHARPIN (Cell Signaling Technology). HOIP was detected in mouse lung tissue by use of a polyclonal antiserum as described elsewhere (1). Horseradish peroxidase-conjugated secondary goat anti-mouse and anti-rabbit antibodies were purchased from Bio-Rad or Cell Signaling Technology. Live/Dead eFluor506 viability dye was purchased from eBioscience. Fluorochrome-labeled mouse antibodies against CD45-FITC (clone: 30-F11), CD11b-eFlour450 (clone: M1/70), CD326-APC (EpCAM) (clone: G8.8), and CD31-PE (PECAM-1) (clone: 390) were purchased from Thermo Fischer, fluorochrome-labeled mouse anti-Na,K-ATPase α_1-AlexaFluor488 (clone: C464.6) was purchased from EMD Millipore, and Podoplanin (T1α) (clone: 8.1.1). All cell culture reagents were purchased from Corning Life Sciences. Protein A/G PLUS-Agarose beads were purchased from Santa Cruz Biotechnology. All other chemicals were purchased from Sigma-Aldrich and were of the highest grade available.

Hypoxia exposure. *In vitro* hypoxic conditions (1.5% O_2, 93.5% N_2, and 5% CO_2) were achieved as described elsewhere (2) by equilibrating the medium in a humidified workstation In Vivo 300 (Baker Ruskinn), which contains an oxygen sensor to continuously monitor the oxygen tension of the chamber. For *in vivo* exposure, WT and *Cre^{SPC}/HOIL-1L$^{fl/fl}$* mice were kept in room air (21% O_2) or exposed to hypoxia (7% O_2) for up to 14 days in a workstation C-Shuttle chamber (Biospherix) with a 14:10-hour light-dark cycle (3). Food and water were available ad libitum. Oxygen and carbon dioxide levels in the chamber were continuously monitored while the chamber temperature was maintained between 20°C and 26°C. At the end of the exposure mice were euthanized, and peripheral tissue was harvested from perfused lungs. Tissue was homogenized in lysis buffer containing 300 mM Mannitol and 12 mM HEPES as described elsewhere (4). Protein quantification and Western blot were performed as described below.

Adenoviral infection. On day 2, rat ATII cells were infected with an HA-tagged adenovirus carrying a dominant-negative, kinase-dead (K45R) variant of the AMPK α_1 subunit (Ad-HA-DN AMPK-α_1; dose, 20 plaque-forming units [pfu] per cell) (5). After 2 h of incubation, DMEM supplemented with 10% fetal bovine serum, 100 U/mL penicillin, and 100 µg/mL streptomycin was added to the cell culture plates. Experiments were performed 24 h later.

Adenoviral production of GFP-Na,K-ATPase α_1-WT and α_1-S18A followed by two rounds of plaque purification was performed by Viraquest, Inc., which provided viral titers and excluded wild-type viral contamination of the viral vectors (negative PCR for glycoprotein E1). WT or *Cre^{SPC}/HOIL-1L$^{fl/fl}$* mice were infected with adenovirus

GFP-Na,K-ATPase α_1-WT (1×10^9 pfu per mouse) or Ad-GFP-Na,K-ATPase α_1-S18A (1×10^9 pfu per mouse) in 50% surfactant vehicle as described elsewhere (6) and housed in a containment facility. After 72 h mice were exposed to hypoxia or kept in room air.

Na,K-ATPase protein abundance and activity. After the corresponding *in vitro* treatments, Na,K-ATPase protein abundance at the plasma membrane was determined by cell surface labeling. Cells were labeled for 20 min using 1 mg/mL EZ-link NHS-SS-biotin (Thermo Fisher Scientific) as described elsewhere (7). After labeling, the cells were rinsed three times with PBS containing 50 mM glycine to quench unreacted biotin and then lysed. Aliquots (150 µg of protein) were incubated overnight at 4°C with end-over-end shaking in the presence of streptavidin beads. The beads were thoroughly washed and proteins were analyzed by SDS-PAGE and Western blot using an α_1-Na,K-ATPase–specific antibody .

The α_1-Na,K-ATPase abundance in the plasma membrane of mouse ATII cells was assessed by flow cytometry. A single cell suspension of lung cells isolated as described above was enriched in AEC using CD326 beads (Miltenyi Biotec) according to the manufacturer instructions. A total of 5×10^6 cells were stained with a mixture of fluorochrome-labeled antibodies (CD45, EpCAM, CD31, and Na,K-ATPase α_1) for 15 min at 4°C in MACS buffer (Miltenyi Biotec). Multicolor flow cytometry was performed by means of a Fortessa flow cytometer (BD Biosciences) as described elsewhere (8). ATII cells were identified as $CD45^-/CD31^-/EpCAM^+$, and Na,K-ATPase α_1 expression was analyzed in that population. Compensation and data analysis were performed using FlowJo software (TreeStar). Data are represented as mean fluorescense intensity.

A high-sensitivity ATPase assay kit, which measures P_i released from ATP hydrolysis, was used according to the manufacturer's instructions (Innova Biosciences). ATPase reactions were performed for 30 min at room temperature in 100 mM Tris (pH, 7.4), 1 mM ATP, and 5 mM Mg^{2+}. Absorbance was read at 600 nm. The Na,K-ATPase activity was determined as the ouabain-sensitive ATPase activity.

Isolation of Soluble Membrane Fraction. After the correspondent treatments, total membranes were prepared as described previously (9). Briefly, cells were homogenized in buffer containing 1 mM EDTA, 1 mM EGTA, 10 mM Tris-HCl (pH 7.5), 1 µg/ml leupeptin, 100 µg/ml N-tosyl-l-phenylalanine chloromethyl ketone (TPCK), and 1 mM phenylmethylsulfonyl fluoride (PMSF) and centrifuged at 500 × *g* to discard nuclei and debris. The supernatant was then centrifuged at 100,000 × *g* for 1 h at 4°C. The supernatant was designated as cytosol, and the pellet containing the crude membrane fraction was resuspended in homogenization buffer supplemented with 1% Triton X-100 (Sigma-Aldrich) centrifuged at 100,000 × *g* for 30 min at 4°C. The supernatant was designated as soluble membrane fraction. The purity of the isolated soluble membrane fraction was tested by immunoblot using a cytosol marker (β-actin).

cDNA and siRNA transfections. Cells were transiently transfected with either FLAG-PKCζ-WT, FLAG-PKCζ-T410A, FLAG-PKCζ-T410E mutants (7), HA-HOIL-1L (10), yellow fluorescent protein (YFP; Addgene) or YFP-tagged PKCζ (10) by use of Lipofectamine 2000 (Life Technologies) according to the manufacturer's recommendation. Experiments were performed 48 h after transfection. Cells were transfected with scrambled, HOIL-1L, HIF-1α (Santa Cruz Biotechnology), or HOIP (QIAGEN) siRNA by use of Lipofectamine RNAiMAX (Life Technologies) according to the manufacturer's recommended protocol, and experiments were performed 24 h later.

Western blot analysis. Proteins were quantified by Bradford assay (Bio-Rad) and resolved in 7.5%–12.5% polyacrylamide gels (SDS-PAGE) and transferred onto nitrocellulose membranes by use of Trans Turbo blot (Bio-Rad). Incubation with specific antibodies was performed overnight at 4°C. When more than one primary antibody was used on the same membrane, immunoblots were stripped by incubating for 1 h at 55°C in stripping solution (62.5 mM Tris-HCl, 2% SDS, and 100 mM 2-mercaptoethanol; pH, 6.8). Immunoblots were developed with a chemiluminescence detection kit (PerkinElmer Life Sciences) used as recommended by the manufacturer. The band's signals in the linear range were quantified by densitometry scan (Image J 1.46r, National Institutes of Health) or Image Studio Software (LI-COR Inc., Lincoln, NE).

Immunoprecipitation and co-immunoprecipitation. Cells were placed on ice and washed twice with ice-cold PBS before being lised for 30 min in a low-detergent lysis buffer containing 150 mM NaCl, 20 mM HEPES, 0.1% NP-40, 5% glycerol, 2 mM EGTA, 2 mM EDTA, 1 mM NaF, 1 mM Na_3VO_4, 1 mM PMSF, 100 μg/mL TPCK, and 1 μg/mL leupeptin (pH, 7.4). The cell extract was obtained by centrifugation at 18,000 *g* for 15 min. When the membrane fraction was used as a source of proteins, they were solubilized in low-detergent lysis instead of the solubilization buffer described above. Equal amounts of cell extract (~1 mg) or soluble membrane fraction proteins (~0.1 mg) were mixed with 2 μL of the corresponding antibody and 40 μL of Protein A/G Plus-agarose beads (Santa Cruz Biotechnology) and incubated overnight at 4°C. The immune complexes were washed three times with low-detergent lysis buffer, and proteins were eluted from the beads and re-suspended in 2× Laemmli sample buffer and analyzed by Western blot.

Cell viability analysis. Cell death was measured using an LDH assay (Roche Applied Science) according to the manufacturer's instructions.

Measurement of oxygen consumption. Oxygen consumption rate (OCR) was determined using an XF96 extracellular flux analyzer (Seahorse Bioscience) (11). Rat ATII cells were plated in Seahorse 96-well plates at a density of 1×10^5 cells per well. On day 2, cells were exposed to hypoxia or kept at normoxia. Coupled OCR was determined as basal OCR minus OCR after treatment with oligomycin (2.5 μM).

Intracellular ATP levels. Intracellular ATP content determination was performed using the Bioluminescence Assay Kit HS II (Sigma) according to the manufacturer's instructions. In brief, after treatment cells were rapidly

rinsed with ice-cold PBS, trypsinized, pelleted, and resuspended in PBS. The same volume of the cell lysis reagent was added and lysates were incubated at room temperature for 5 min. After transferring the lysates to a white microtiter plate (Thermo Fisher), luminescence was measured immediately after the addition of the luciferase. A standard curve was generated on the same plate.

Gene expression profiling (RNA-seq) and bioinformatic analysis. Mouse ATII cells were sorted as described in the Experimental Procedures section and were immediately lysed with RLT Plus buffer from a Qiagen RNeasy Plus Mini kit (Qiagen) containing 1% β-mercaptoethanol. RNA isolations were performed using a Qiagen RNeasy Plus Mini kit (Qiagen). Four biological replicates were used for each genotype/condition. RNA quality and quantity were measured using the TapeStation 4200 instrument (Agilent Technologies). NEBNext Ultra RNA (New England Biolabs) was used for full-length cDNA synthesis and library preparation. DNA libraries sequencing was performed using an Illumina NextSeq 500 instrument (Illumina) of the average dept of 5–7.5 million aligned reads per sample.
Northwestern's High Performance Computing Cluster (Quest) was used to analyze the RNA-Seq data. Reads were demultiplexed using bcl2fastq (Version 2.17.1.14), quality of the reads was checked using fastqc (Version 0.11.5). Reads were trimmed using trimmomatic (Version 0.33) and aligned to reference mouse genome mm10 using Tophat (Version 2.1.0). Read counts for the genes were quantified using HTSeq (Version 0.6.1). The counts were used for gene-level differential expression analysis using edgeR (R/Bioconductor package) (12). Gene ontologies were evaluated using GORILLA (13).

Bronchoalveolar lavage fluid and permeability determination. After treatments, BALF was collected for cell counts, protein quantification, and permeability determination. The bronchoalveolar lavage was performed through a 20-gauge angiocath ligated into the trachea. A 1 mL aliquot of PBS was instilled into the lungs and then carefully aspirated three times as described elsewhere (4).

Lung permeability was assessed as described elsewhere (14). In brief, 125 µL of fluorescein isothiocynate (FITC)–dextran (Sigma-Aldrich; MW, 4000; concentration, 0.05 g/mL) was delivered into the retro-orbital plexus to anesthetized mice. The mice were kept sedated for 30 min. immediately after BALF collection, 400 µL of blood was collected from the right ventricle into a syringe containing 50 µL of sodium citrate (3.2%). Relative lung permeability was estimated from the ratio of the fluorescence in the BALF to that in the plasma, which were measured using a microplate reader (Corning; excitation, 488 nm; emission, 530 nm).

Histology. Lungs were removed and fixed with 4% paraformaldehyde. Lungs were processed and embedded, and 4 µm cross-sections were stained with hematoxylin and eosin (H&E) or assayed by terminal deoxynucleotidyl transferase–mediated deoxyuridine triphosphate nick end labeling (TUNEL). Brightfield images of lungs were obtained using TissueFAXS software (TissueGnostics). Serial H&E images were stitched into a high-resolution macroscopic montage. The alveolar septa area was quantified in H&E images using FIJI software, and TUNEL quantification was performed using HistoQuest 4.0.4.0150 (TissueGnostics).

Statistics. The Student *t* test was used for single comparisons and analysis of variance (ANOVA) for multiple comparisons. All analyses were performed using GraphPad Prism version 7.0 (GraphPad Software). All data are expressed as mean ± SD (n = 3) unless otherwise indicated. A *p*-value of <0.05 was considered to be statistically significant for all tests.

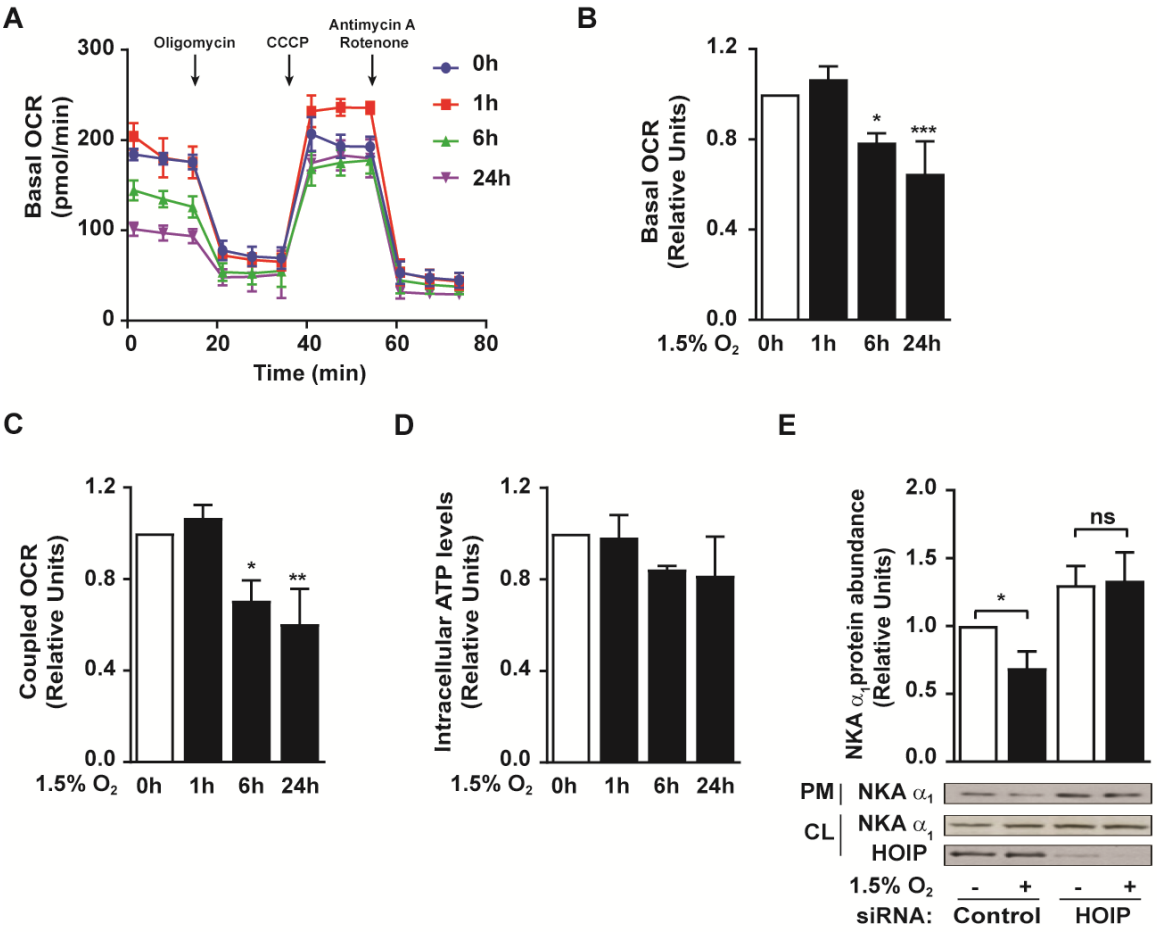

Figure S1. A-C) Oxygen consumption rate (OCR) of intact rat ATII cells exposed to normoxia or hypoxia (1.5% O_2) for up to 24 h. A) Representative tracings of OCR B) Basal OCR from rat ATII cells exposed to hypoxia compared to the OCR of normoxic rat ATII cells. Graph bars represent mean ± SD (n = 3). Statistical significance was calculated using one-way ANOVA and the Tukey multiple comparisons test (*$p < 0.05$, ***$p < 0.001$). C) Relative coupled OCR, determined as basal OCR minus OCR after treatment with oligomycin (2.5 μM). Graph bars represent mean ± SD (n = 3). Statistical significance was calculated using one-way ANOVA and the Tukey multiple comparisons test (*$p < 0.05$, **$p < 0.01$). D) Intracellular ATP levels measured in rat ATII cells exposed to hypoxia compared to normoxia. E) A549 cells were transfected with scrambled (control) or HOIP siRNA (HOIP) and exposed to normoxia or hypoxia for 24 h, then plasma membrane proteins were isolated after cell surface labeling with biotin and immunoblotted with $α_1$-Na,K-ATPase (NKA $α_1$)–specific antibody. Densitometry quantification of immunoblots of $α_1$-Na,K-ATPase in relation to cell lysate $α_1$-Na,K-ATPase is shown. Graph bars represent mean ± SD (n = 3).

Statistical significance was calculated using one-way ANOVA and the Tukey multiple comparisons test (*$p < 0.05$).

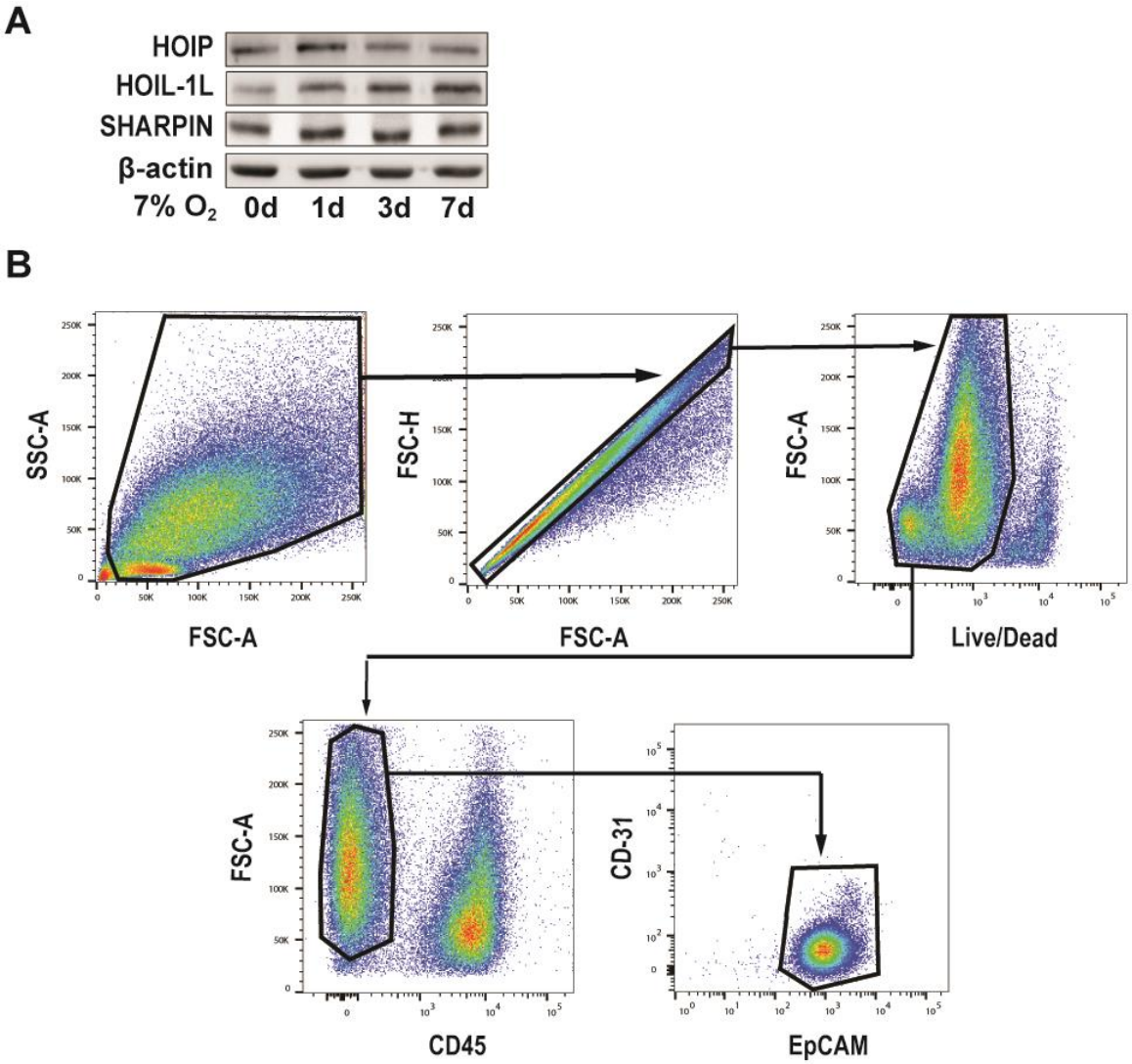

Figure S2. A) WT mice were kept in room air (0 d) or exposed to 7% O_2 for 7 days, and protein levels in lung peripheral tissue homogenates were analyzed by Western blot. Representative immunoblots are shown (n = 4). B) Gating strategy used to identify mouse ATII cells. After excluding doublets and dead cells, and followed by exclusion of cells of hematopoietic origin identified as $CD45^+$ cells, ATII cells were identified as $CD31^-EpCAM^+$ cells.

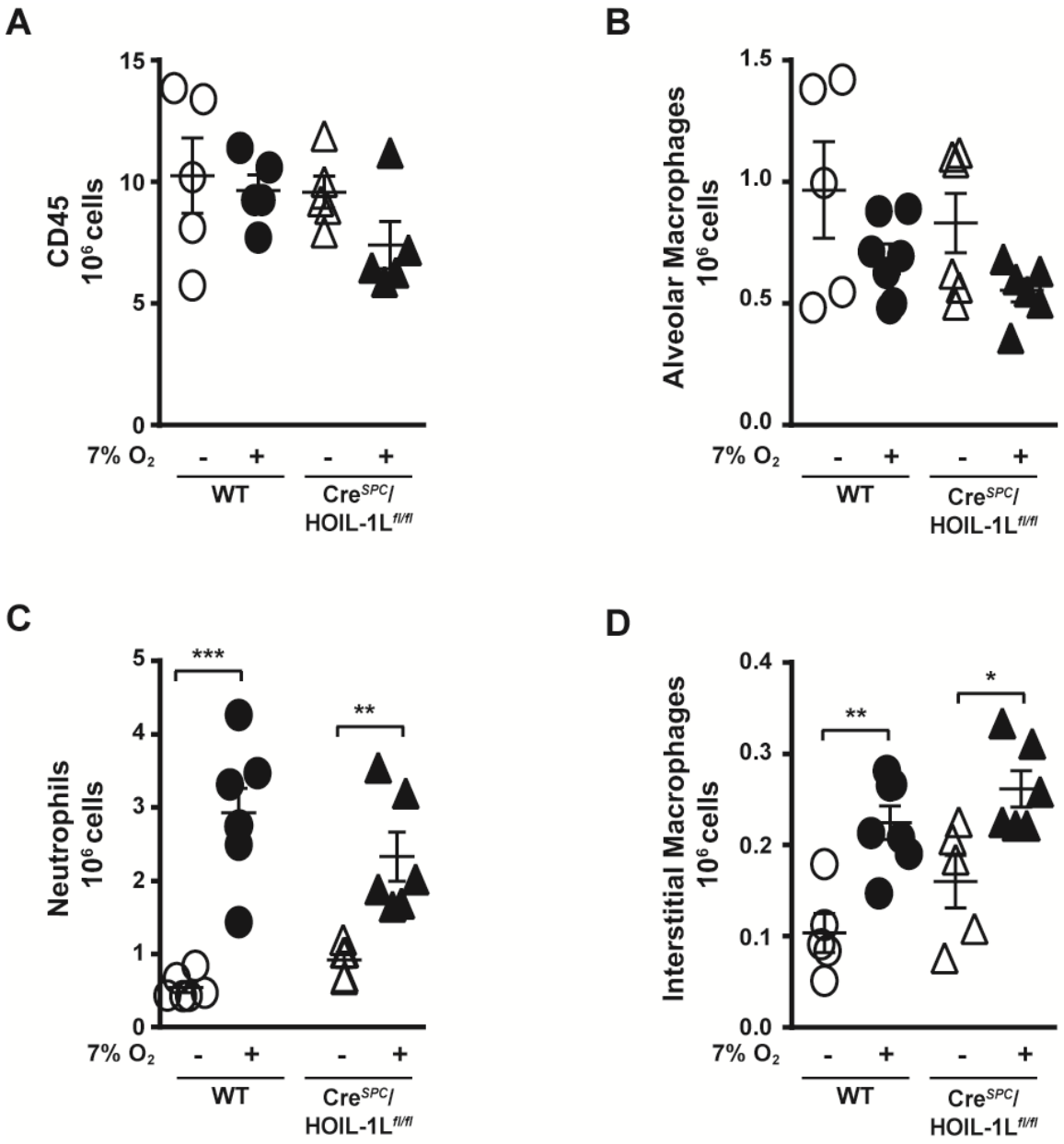

Figure S3. WT (circles) and Cre^{SPC}/HOIL-1L$^{fl/fl}$ (triangles) mice were kept in room air (white) or exposed to 7% O_2 for 7 days (black). Shown are the number of A) CD45$^+$ cells, B) neutrophils, C) alveolar macrophages, and D) interstitial macrophages, as assessed by flow cytometry. Graph data represent mean ± SD (n = 6). Statistical significance was calculated using one-way ANOVA and the Tukey multiple comparisons test (*p < 0.05, **p < 0.01, ***p < 0.001).

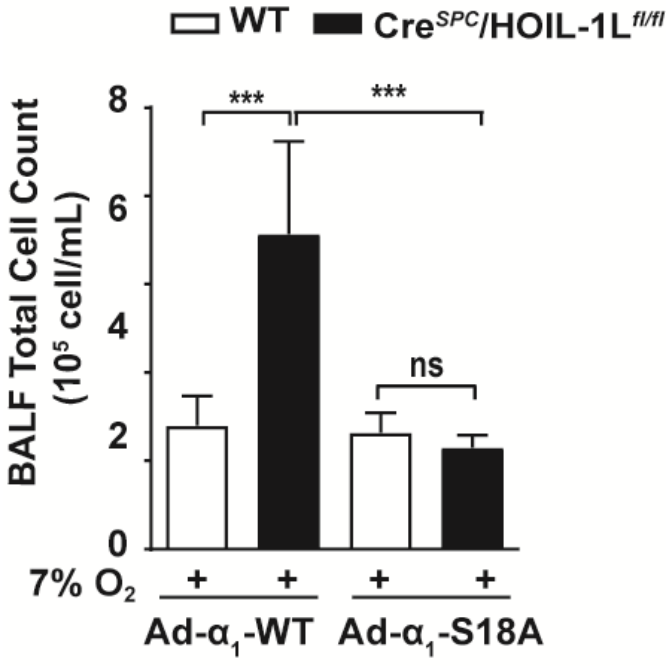

Figure S4. WT (white bars) and Cre^{SPC}/HOIL-$1L^{fl/fl}$ (black bars) mice were infected with either adenovirus expressing GFP-Na,K-ATPase α_1-WT (Ad-α_1-WT) or GFP-Na,K-ATPase α_1-S18A (Ad-α_1-S18A) and exposed to 7% O_2 for 7 days and total cell count was measured in BALF as described in Experimental Procedures (n = 5).

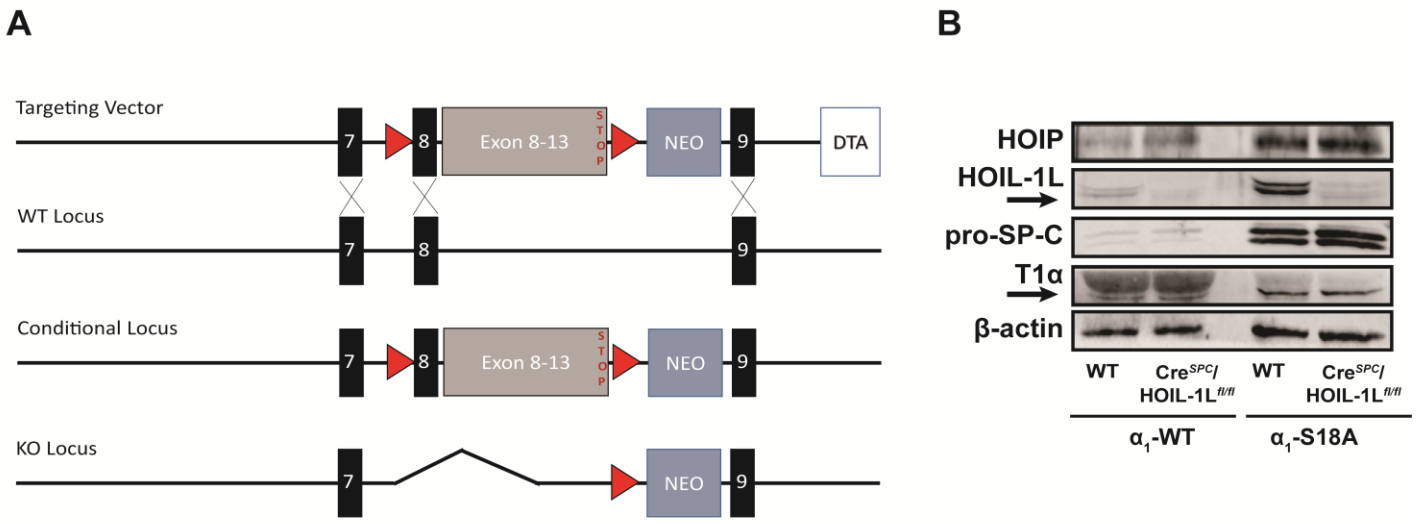

Figure S5. A) Generation of a mouse strain in which HOIL-1L was ablated in a conditional manner. The structures of the HOIL1-L genomic allele, the targeting vector, and the mutated allele are shown. B) ATI and ATII cells were isolated from WT and Cre^{SPC}/HOIL-$1L^{fl/fl}$ mice by FACS. ATI cells were identified as $T1\alpha^{+}EpCAM^{+}CD31^{-}$ and ATII cells were identified as $EpCAM^{+}T1\alpha^{-}$ $CD31^{-}$ cells. Equal amount of cell lysate proteins (30 µg) was analyzed by Western blot using the indicated antibodies. β-actin was used as loading control. Arrows indicate non specific bands.

Table S1. Differentially expressed genes in ATII cells isolated from WT and Cre^{SPC}/HOIL-1L$^{fl/fl}$ mice in normoxic conditions.

Parameter	Value
Comparison	Normoxia WT vs. *Cre^{SPC}/HOIL-1L$^{fl/fl}$*
No. of genes	
Total	13,617
Upregulated	13
Downregulated	7
Genes	
Upregulated	*Zmiz1; Meg3; Bach1; Notch2; Golgb1; Ahdc1; Ppl; Tnrc18; Trim56; Trrap; Foxo3; Rnf213; Wdfy1*
Downregulated	*Aqp1; Srgn; Mrps24; Areg; Hist1h1c; Pax1; Sprr1a*

The data reported in this paper have been deposited in the Gene Expression Omnibus (GEO) database,

https://www.ncbi.nlm.nih.gov/geo/query/acc.cgi?acc=GSE102107

References

1. Kirisako T, Kamei K, Murata S, Kato M, Fukumoto H, Kanie M, Sano S, Tokunaga F, Tanaka K, Iwai K (2006) A ubiquitin ligase complex assembles linear polyubiquitin chains. *EMBO J* 25(20):4877-4887.
2. Dada L A, Chandel N S, Ridge K M, Pedemonte C, Bertorello A M, Sznajder J I (2003) Hypoxia-induced endocytosis of Na,K-ATPase in alveolar epithelial cells is mediated by mitochondrial reactive oxygen species and PKC-ζ. *J. Clin. Invest.* 111:1057-1064.
3. Litvan J, Briva A, Wilson M S, Budinger G R S, Sznajder J I, Ridge K M (2006) beta -Adrenergic receptor stimulation and adenoviral overexpression of sod2 prevent the hypoxia-mediated decrease in Na,K-ATPase and alveolar fluid reabsorption. *J. Biol. Chem.* 281:19892-19898.
4. Brazee P L, Soni P N, Tokhtaeva E, Magnani N, Yemelyanov A, Perlman H R, Ridge K M, Sznajder J I, Vagin O, Dada L A (2017) FXYD5 Is an Essential Mediator of the Inflammatory Response during Lung Injury. *Front Immunol* 8:623.
5. Vadasz I, Dada L A, Briva A, Trejo H E, Welch L C, Chen J, Toth P T, Lecuona E, Witters L A, Schumacker P T, Chandel N S, Seeger W, Sznajder J I (2008) AMP-activated protein kinase regulates CO2-induced alveolar epithelial dysfunction in rats and human cells by promoting Na,K-ATPase endocytosis. *J Clin Invest* 118(2):752-762.
6. Lubarski-Gotliv I, Asher C, Dada L A, Garty H (2016) FXYD5 Protein Has a Pro-inflammatory Role in Epithelial Cells. *J Biol Chem* 291(21):11072-11082.
7. Gusarova G A, Dada L A, Kelly A M, Brodie C, Witters L A, Chandel N S, Sznajder J I (2009) Alpha1-AMP-activated protein kinase regulates hypoxia-induced Na,K-ATPase endocytosis via direct phosphorylation of protein kinase C zeta. *Mol Cell Biol* 29(13):3455-3464.
8. Peteranderl C, Morales-Nebreda L, Selvakumar B, Lecuona E, Vadasz I, Morty R E, Schmoldt C, Bespalowa J, Wolff T, Pleschka S, Mayer K, Gattenloehner S, Fink L, Lohmeyer J, Seeger W, Sznajder J I, Mutlu G M, Budinger G R, Herold S (2016) Macrophage-epithelial paracrine crosstalk inhibits lung edema clearance during influenza infection. *J Clin Invest* 126(4):1566-1580.
9. Ridge K M, Dada L, Lecuona E, Bertorello A M, Katz A I, Mochly-Rosen D, Sznajder J I (2002) Dopamine-induced exocytosis of Na,K-ATPase is dependent on activation of protein kinase C-epsilon and -delta. *Mol Biol Cell* 13(4):1381-1389.
10. Queisser M A, Dada L A, Deiss-Yehiely N, Angulo M, Zhou G, Kouri F M, Knab L M, Liu J, Stegh A H, DeCamp M M, Budinger G R, Chandel N S, Ciechanover A, Iwai K, Sznajder J I (2014) HOIL-1L functions as the PKCzeta ubiquitin ligase to promote lung tumor growth. *Am J Respir Crit Care Med* 190(6):688-698.
11. Martinez-Reyes I, Diebold L P, Kong H, Schieber M, Huang H, Hensley C T, Mehta M M, Wang T, Santos J H, Woychik R, Dufour E, Spelbrink J N, Weinberg S E, Zhao Y, DeBerardinis R J, Chandel N S (2016) TCA Cycle and Mitochondrial Membrane Potential Are Necessary for Diverse Biological Functions. *Mol Cell* 61(2):199-209.
12. McCarthy D J, Chen Y, Smyth G K (2012) Differential expression analysis of multifactor RNA-Seq experiments with respect to biological variation. *Nucleic Acids Res* 40(10):4288-4297.
13. Eden E, Navon R, Steinfeld I, Lipson D, Yakhini Z (2009) GOrilla: a tool for discovery and visualization of enriched GO terms in ranked gene lists. *BMC Bioinformatics* 10:48.
14. Soberanes S, Urich D, Baker C M, Burgess Z, Chiarella S E, Bell E L, Ghio A J, De Vizcaya-Ruiz A, Liu J, Ridge K M, Kamp D W, Chandel N S, Schumacker P T, Mutlu G M, Budinger G R (2009) Mitochondrial complex III-generated oxidants activate ASK1 and JNK to induce alveolar epithelial cell death following exposure to particulate matter air pollution. *J Biol Chem* 284(4):2176-2186.